ORIGINAL PAPER

Effect of heat treatment on electrochromic properties of TiO$_2$ thin films

Shih-Yuan Lin · Ying-Chung Chen · Chih-Ming Wang · Chan-Chih Liu

Abstract Electrochromic titanium oxide (TiO$_2$) films were deposited on ITO/glass substrates by chemical solution deposition (CSD). The stock solutions were spin-coated onto substrates and then heated at various temperatures (200–500 °C) in various oxygen concentrations (0–80%) for 10 min. The effects of the processing parameters on the electrochromic properties of TiO$_2$ films were investigated. X-ray diffraction measurements demonstrated that the amorphous TiO$_2$ films were crystallized to form anatase films above 400 °C. The electrochromic properties and transmittance of TiO$_2$ films were measured in 1 M LiClO$_4$–propylene carbonate (PC) non-aqueous electrolyte. An amorphous 350 nm-thick TiO$_2$ film that was heated at 300°C in 60% ambient oxygen exhibited the maximum transmittance variation (ΔT%), 14.2%, between the bleached state and the colored state, with a ΔOD of 0.087, Q of 10.9 mC/cm^2, η of 7.98 cm^2/C and x in Li$_x$ClO$_4$ of 0.076 at a wavelength (λ) of 550 nm.

S.-Y. Lin · Y.-C. Chen (✉)
Department of Electrical Engineering,
National Sun Yat-Sen University,
No.70, Lien Hai Rd.,
Kaohsiung 804 Taiwan, Republic of China
e-mail: ycc@mail.ee.nsysu.edu.tw

C.-M. Wang · C.-C. Liu
Department of Electrical Engineering, Cheng Shiu University,
No. 840, Chengcing Rd., Niaosong Township,
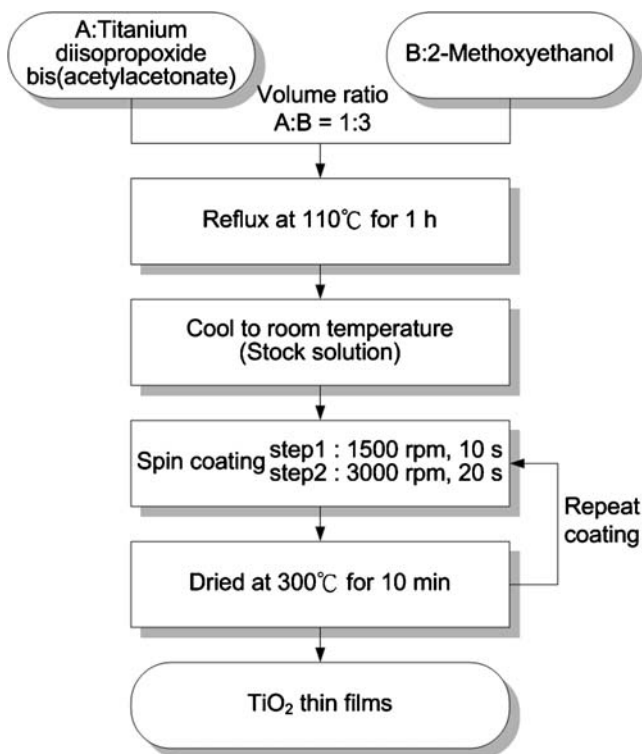Kaohsiung 833 Taiwan, Republic of China

Introduction

Recently, TiO$_2$ films have been studied as counter electrodes (CE) because their microstructural features favor ion transportation. Li-doped TiO$_2$ electrodes have been demonstrated to be useful in photoelectrochemical solar cells and Li ion batteries [1, 2]. During the cyclic voltammetry (CV) of propylene carbonate (PC), applying a cathodic potential changed the transmittance of TiO$_2$ films from a transparent state to blue, indicating electrochromic properties. The electrochromic properties of almost all transition metal oxides have been studied because of their potential applications in electrochromic devices (ECDs) such as displays, smart windows, sunroofs, and rearview and car mirrors, since they can, applying a voltage pulse, reversibly change their color [3–7]. These oxides can be colored anodically (NiO$_x$, IrO$_2$, Rh$_2$O$_3$) or cathodically (WO$_3$, MoO$_3$, TiO$_2$). TiO$_2$ is a member of the cathodic coloration class. The widely accepted model of the electrochromic reaction is the double injection of electrons and monovalent ions into the oxide matrix, as follows: [8]

$$\text{TiO}_2 + x(\text{M}^+ + \text{e}^-) \rightleftarrows \text{M}_x\text{TiO}_2 \atop \text{(transparent)} \qquad \text{(blue)} \tag{1}$$
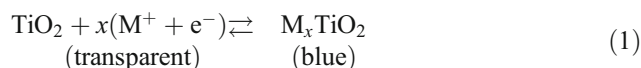
where M$^+$ can be H$^+$ or Li$^+$. The insertion coefficient, x, can saturate at a value of one depending on the microstructure of the deposited thin film.

Since the electrochromic properties are strongly related to the microstructure and the surface morphology of the films, the synthesis of crystalline TiO$_2$ films has attracted interest in recent years. However, the amorphous TiO$_2$ film has a greater charge capacity and higher coloration efficiency than an anatase TiO$_2$ film because it has a more open microstructure [9, 10]. The goal of this study is to prepare amorphous and anatase TiO$_2$ films by chemical solution

Fig. 1 Flow diagram of synthesis of electrochromic TiO_2 thin films

Fig. 3 Thermogravimetric analysis data (TGA) and corresponding DTA data for TiO_2 gel

deposition (CSD). This technique has several advantages such as high homogeneity, precise compositional control and low cost, without the use of a high vacuum [11, 12]. This study discusses the effect of the amorphous and the anatase phases on the electrochromic properties of TiO_2 film. The dependence of the optical characteristics of an electrochromic TiO_2 film on its thickness is also considered.

oxide bis(acetlyacetonate), $((CH_3)_2CHO)_2Ti(C_5H_7O_2)_2$, was used as the source material and 2-methoxyethanol, $CH_3OCH_2CH_2OH$, was used as the solvent. The volume ratio of the TiO_2 source to the solvent was 1:3 to ensure adhesion of the stock solution to the substrate. The mixed solution was refluxed at 110 °C for 1 h in air and then cooled to room temperature. The stock solution was thus obtained. The stock solution was spin-coated on ITO/glass substrates using a commercial photoresist spinner. The transparent and conductive ITO coated glass substrates with dimensions of 3×3.5 cm^2, sheet resistance of 15 Ω/sq. and transmittance of 85%. The spin rate of the first step was 1,500 rpm for 10 s and the following step was 3,000 rpm for 20 s. TiO_2 wet films were heated at various temperatures (200–500°C) in various concentrations of oxygen (0–80%) for 10 min in a rapid thermal process (RTP, heating rate=1 °C/s). In

Experimental

Preparation of TiO_2 thin films by CSD

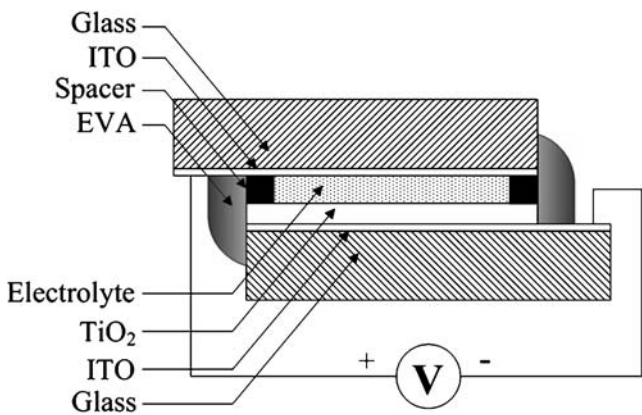Figure 1 shows a flow diagram of the preparation of electrochromic TiO_2 films by the CSD method. Titanium diisoprop-

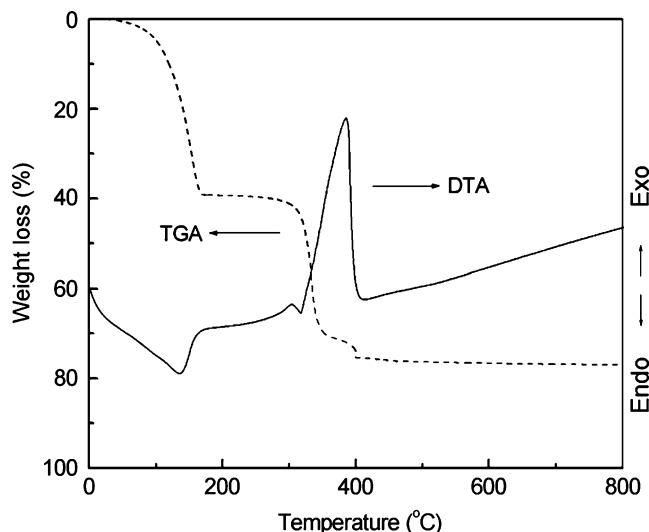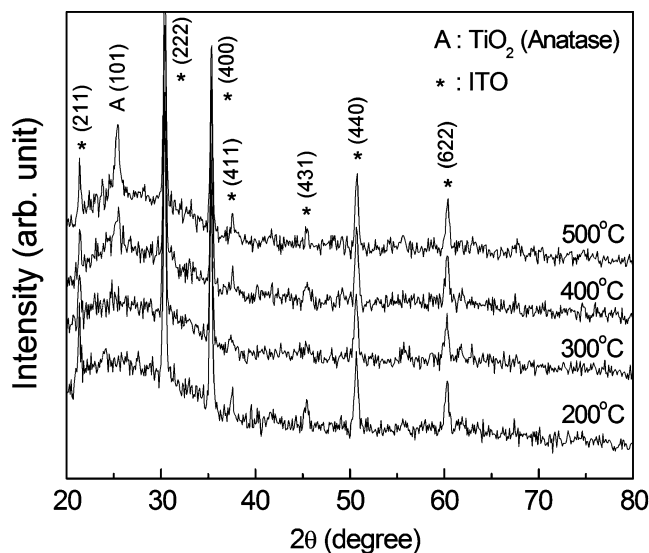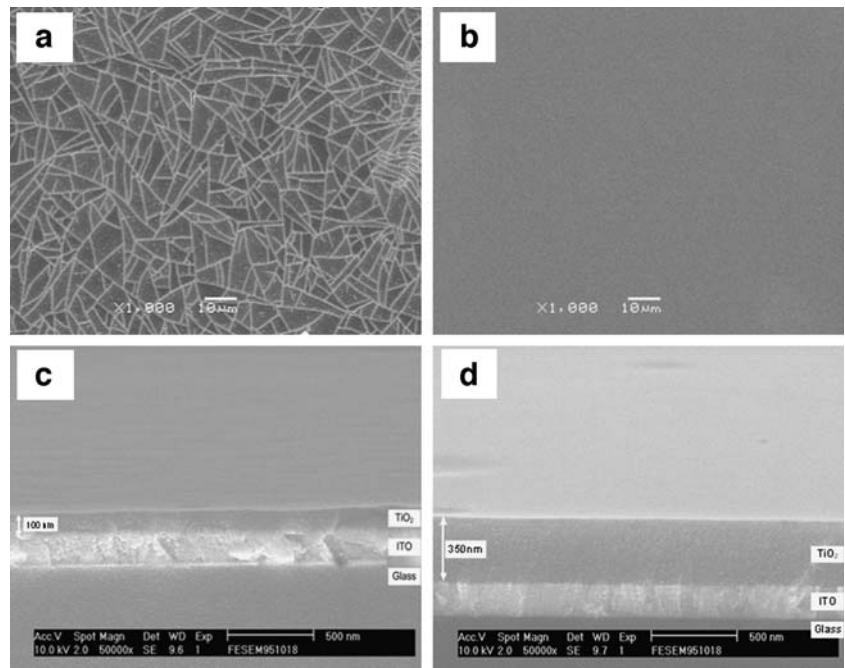Fig. 2 Schematic configuration of electrochromic device (ECDs)

Fig. 4 XRD patterns of TiO_2 thin films heated at various temperatures

Fig. 5 SEM images of TiO$_2$ thin films heated at 300 °C for 10 min using **a** hot plate and **b** RTP, and cross-sectional views of the **c** 100 nm and **d** 350 nm TiO$_2$ films

addition, the RTP by an infrared gold image furnace will be adopted for the heating treatments of TiO$_2$ thin films. The RTP technology has been widely used in the semiconductor industry. This method has several advantages such as short heating time, rapid grain growth and avoids strains or reactions at the film–substrate interface and results in a dense microstructure [13, 14]. Various heat treatments were also performed at 300 °C for 10 min using a hot plate and RTP, respectively. The thicknesses of the TiO$_2$ films were very sensitive to the conditions of deposition including the concentration of the stock solution, the spin rate and the number of cycles in spin-coating/heating processes. In this study, the coating/heating operations were repeated until the desired thickness 100 or 350 nm) was obtained.

Fabrication and measurement of ECD devices

The thermal decomposition of the stock solution at various temperatures was examined by thermogravimetric analysis (TGA) and differential thermal analysis (DTA) at a heating rate of 10°C/min. Crystal structures of TiO$_2$ films were analyzed by X-ray diffraction (XRD, Siemens D-5000) with Cu-Kα radiation. The thickness and surface microstructures of the TiO$_2$ films were examined using a scanning electron microscope (SEM, JEOL JSM-6300). The electrochemical behaviors (cyclic voltammograms, CVs) of the films were examined using an electrochemical analyzer (CHI-611B) by immersing the sample in an electrolyte of 1 M LiClO$_4$ in PC. The CV measurements from +2.0 V to −3.8 V were made using potential sweeps of 50 mV/s. Ultraviolet–Visible (UV–Vis) spectra were obtained to measure the transmittance of each deposited specimen which was colored at −3.8 V and bleached at +2.0 V using a Jasco, V-570 spectrometer over the wavelength range 300–700 nm. The transmittance variation ($\Delta T\%$) is given by $\Delta T\% = T_{\text{Bleached}} - T_{\text{Colored}}$, where T_{Bleached} and T_{Colored} represent the transmittance at a wavelength (λ) of 550 nm in the bleaching and the coloring states, respectively. The change in the optical density (ΔOD) is given by ΔOD$=\log(T_{\text{Bleached}}/T_{\text{Colored}})$ at a λ of 550 nm.

Table 1 The process parameters and measurement results of TiO$_2$ thin films

The process parameters and measurement results of TiO$_2$ thin films

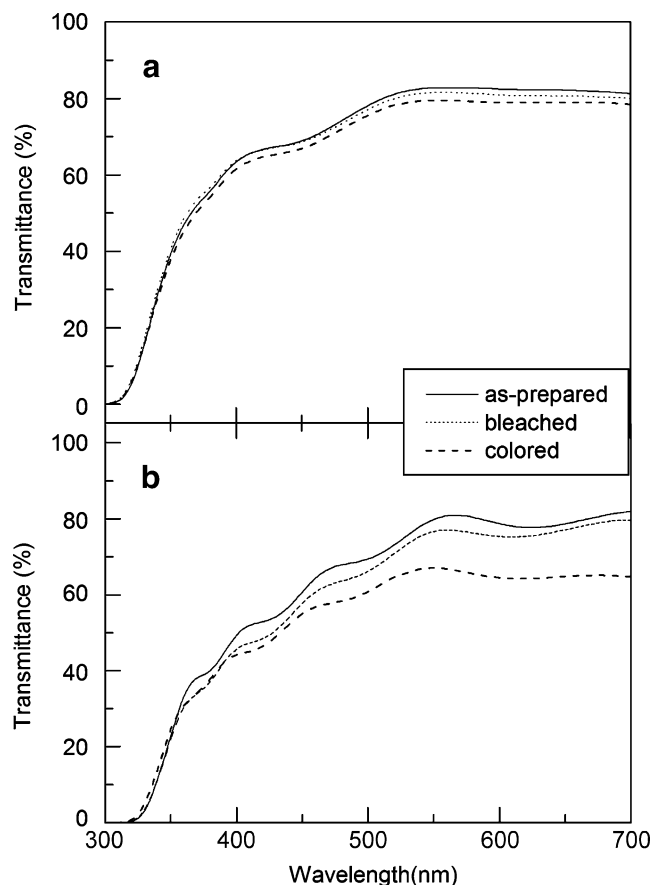| Thickness (nm)	100	350	350	350	350	350	350	350
O$_2$ (%)	0	0	40	60	80	60	60	60
Temperature (°C)	300	300	300	300	300	200	400	500
$T_{\text{As-prepared}}$ (%)	80.36	79.82	81.73	81.78	80.77	78.25	81.19	77.62
T_{Bleached} (%)	79.97	76.65	79.62	77.98	76.65	76.46	78.21	77.12
T_{Colored} (%)	78.62	67.06	65.83	63.78	66.36	75.57	67.19	73.2
ΔT (%)	1.35	9.59	13.79	14.2	10.29	0.89	11.02	3.92
ΔOD	0.007	0.058	0.082	0.087	0.062	0.005	0.065	0.022

Fig. 6 Transmittance spectra of **a** 100 nm and **b** 350 nm TiO$_2$ thin films

Figure 2 shows a cross-sectional view of ECDs including the electrochromic TiO$_2$ layer. The device was assembled by separating the ITO/glass and the TiO$_2$/ITO/glass by approximately 1 mm using a spacer. The free volume between the two electrodes was filled with the electrolyte. The entire device with the glass/ITO/electrolyte/TiO$_2$/ITO/glass structure was then sealed using ethylene vinyl acetate (EVA). This method is convenient optically characterizing an electrochromic TiO$_2$ film.

Results and discussion

Figure 3 plots the thermolysis behavior of TiO$_2$ gel. TGA analysis indicates that two major weight losses occurred at about 400 °C. The gel exhibited an approximately 80%-weight-loss over in the temperature range 100–400 °C by the elimination of adsorbed water and solvent (2-methoxyethanol whose b.p. is 122 °C) and the oxidation of the organic substances. The endothermic peaks at about 135 °C and 320 °C are associated with earlier weight losses. The amorphous-to-anatase phase transformation in TiO$_2$ is responsible for the exothermic peak at about 386 °C. These results are consistent with the values in the literature [15,

16]. Figure 4 presents the XRD patterns of the TiO$_2$ films heated to temperatures from 200 to 500 °C for 10 min. The film heated to 300 °C remained amorphous. However, crystalline TiO$_2$ films were obtained upon raising the heating temperature to over 400 °C. The crystallization of the TiO$_2$ film is consistent with the TGA/DTA plots, suggesting that the amorphous-to-anatase phase transformation temperature occurs at about 386 °C. Figure 4 also reveals an increase in the crystallinity with heating temperature.

Figure 5 presents SEM micrographs of TiO$_2$ films heated to 300 °C for 10 min using various heat-treatment methods. No microstructural feature of the films heated using a hot plate [Fig. 5a] and RTP [Fig. 5b] could be resolved. However, many cracks appeared on the surface, as shown in Fig. 5a, suggesting that heat treatment of the hot plate causes larger stresses and results in cracking [17]. Figure 5c and d present the uniform TiO$_2$ films that are obtained by RTP with a mean thickness of 100 nm and 350 nm, respectively. The thicknesses of the TiO$_2$ films did not increase significantly as the number of coating/heating cycles increased. Tu et al. [18] found that the ethanol route yielded a single-layer film that was thinner than those obtained by other routes. The coating/heating process was required to yield high-quality thin films of the desired thickness. Table 1 presents the experimental parameters and results.

Figure 6 presents the optical transmittance spectra of the 100 and 350-nm-thick TiO$_2$ films heated at 300 °C for 10 min by RTP. Inserting Li$^+$ ions changes the transmittance of TiO$_2$ films in the wavelength range of 300–700 nm and the color of the film changes reversibly from transparent to blue [19]. The transmittance (at 550 nm) of the 350-nm-thick TiO$_2$ film is varied from approximately 76.65% (bleached state) to 67.06% (colored state), and the corresponding $\Delta T\%$ and ΔOD are 9.59% and 0.058, respectively. Figure 7 plots the CVs of the 100-nm-thick
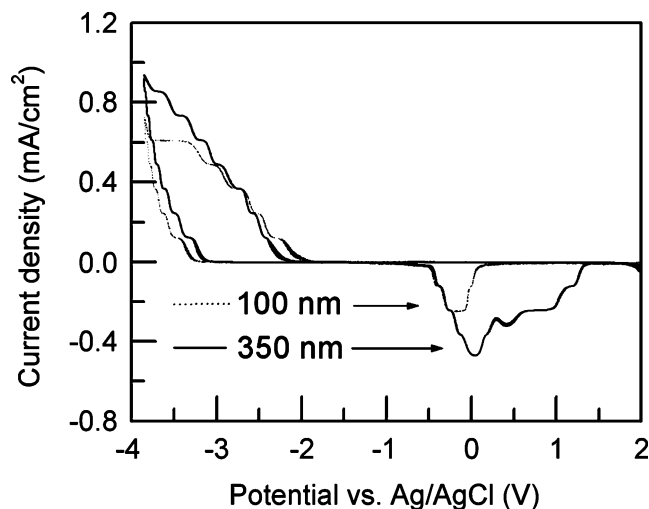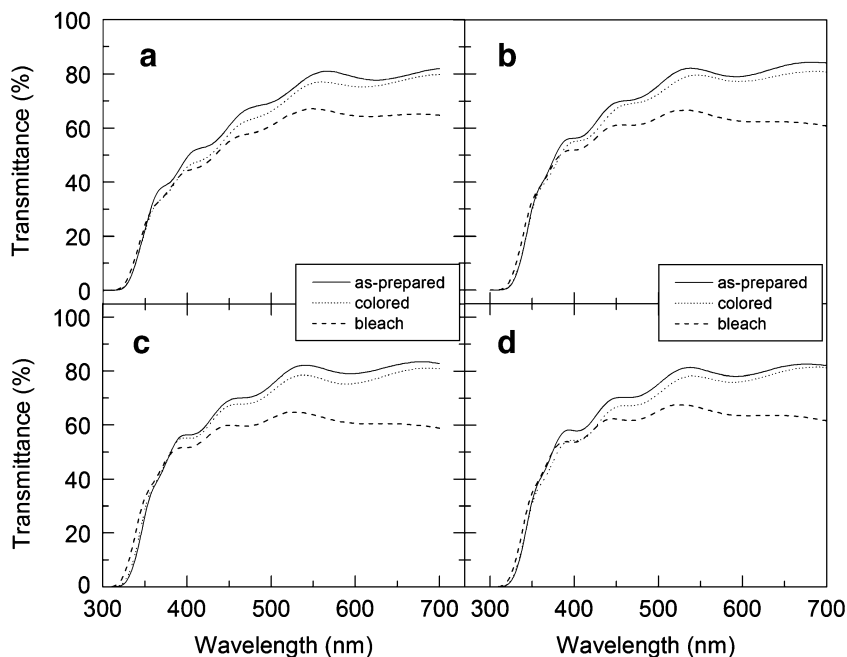

Fig. 7 Cyclic voltammograms of **a** 100 nm and **b** 350 nm TiO$_2$ thin films

Fig. 8 Transmittance spectra of TiO$_2$ thin films heated at 300 °C for 10 min in **a** 0%, **b** 40%, **c** 60% and **d** 80% oxygen

and 350-nm-thick TiO$_2$ films. The 100-nm TiO$_2$ film exhibits a reduction peak at −3.8 V (0.72 mA/cm^2) and an oxidation peak at −0.18 V (−0.24 mA/cm^2). The 350-nm TiO$_2$ film has a reduction peak at −3.8 V (0.94 mA/cm^2) and an oxidation peak at 0.04 V (−0.46 mA/cm^2). This result indicates that the thicker film has a larger charge capacity (amount of Li$^+$ ion intercalation) [10, 20].

Figure 8 presents the transmittance spectra of the TiO$_2$ films relative to the oxygen content (0–80%) during heat treatment. A comparison across oxygen contents indicates that the TiO$_2$ film that was heated in 60% oxygen [Fig. 8c]

had the maximum ΔT%, 14.2% with a ΔOD of 0.087. The oxygen content affects the electrochromic properties of the TiO$_2$ film, which result is associated with the presence of oxygen vacancies and color centers [21–23]. Figure 9 plots the dependence of the transmittance spectra of TiO$_2$ films on the heating temperature (RTP, 200–500°C). ΔT% and ΔOD decreased as the heating temperature increased over 300°C, because many fewer charges are injected into the crystalline TiO$_2$ film than into the amorphous film [24–27]. That is, Li$^+$ ion intercalation in the amorphous TiO$_2$ film is much easier than in the anatase film because the former has

Fig. 9 Transmittance spectra of TiO$_2$ thin films heated at **a** 200 °C, **b** 300 °C, **c** 400 °C and **d** 500 °C in 60% oxygen content for 10 min
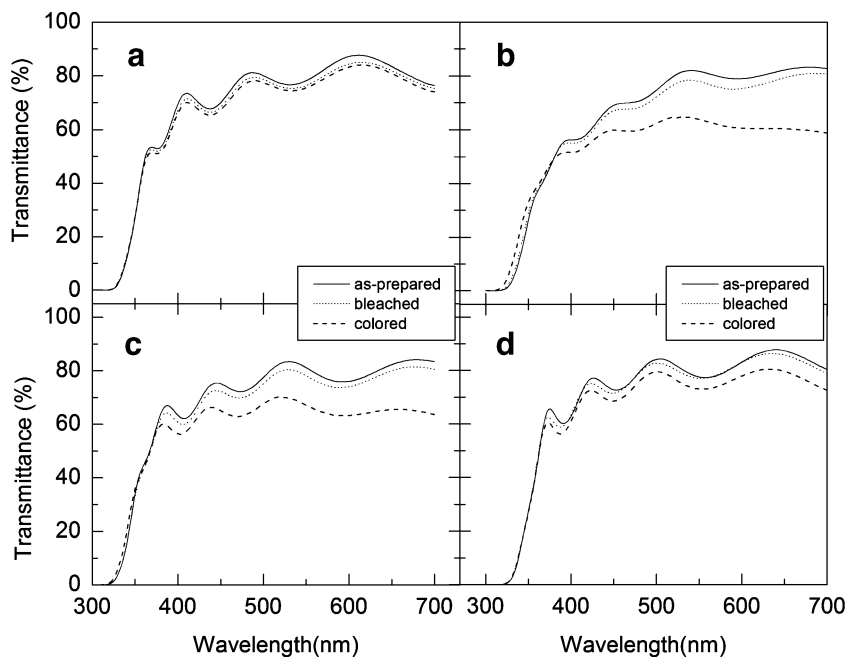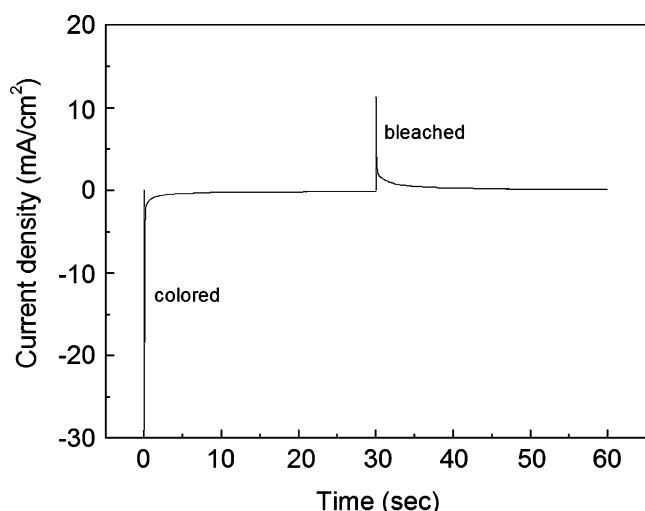
Fig. 10 Current response of 350-nm-thick TiO$_2$ film heated at 300 °C

a much more open microstructure. Figure 10 presents the Li$^+$ ion intercalation/deintercalation charge (Q) in the colored and bleached stable states. First, the degree of coloration is monitored from 0 to 30 s for intercalation and from 30 to 60 s for deintercalation. The amount of charge from 0 to 30 s associated with intercalation during coloration is 10.9 mC/cm^2 and that from 30 to 60 s associated with deintercalated during bleaching is 9.7 mC/cm^2. The transmittance of the TiO$_2$ film in the colored state depends on the intercalated Li$^+$ charge, specified by the insertion coefficient x for the Li$_x$TiO$_2$ compound. Accordingly, the maximum value of x is 0.076 in the colored state and 0.067 in the bleached state. Formulae for the intercalation/deintercalation coefficient x has been detailed elsewhere [10]. The coloration efficiency (η) is defined as $\eta=(\Delta OD/Q)$. When the 350-nm-thick TiO$_2$ film was heated at 300 °C in 60% oxygen, the η value was 7.98 cm^2/C. Accordingly, the experimental η of 7.98 cm^2/C exceeds that of a single-layer TiO$_2$ thin film deposited by rf magnetron sputtering [20].

Conclusions

TiO$_2$ electrochromic films were deposited on ITO/glass substrates by CSD. Additionally, ECDs were prepared for measurement of their optical and electrochromic properties. The phase transformation from the amorphous to the anatase TiO$_2$ film occurs at about 386 °C and the crystallinity increases with the heating temperature. The assembly of ECDs is convenient for electrochemical and optical characterization. As Li$^+$ ions are inserted, the amorphous and anatase TiO$_2$ films become blue and light blue, respectively. In this study, the 350-nm-thick amorphous TiO$_2$ film obtained by RTP at an oxygen concentration of 60% and a heating temperature of 300 °C has favorable electrochromic properties. The following electrochemical properties of TiO$_2$ films were obtained; (a) $\Delta T\%$ was 14.2% (λ at 550 nm), (b) ΔOD was 0.087 (λ at 550 nm), (c) Q was 10.9 mC/cm^2, (d) η was 7.98 cm^2/C, (e) x in Li$_x$ClO$_4$ was 0.076. The amorphous TiO$_2$ films are suggested to be appropriate for ECD by CSD. Furthermore, such a film can be regarded as a buffer layer which increases the adhesion between the TiO$_2$ films (deposited by rf magnetron sputtering) and the ITO/glass substrate, improving the optical and electrochromic properties of ECDs [28].

References

1. Regan BO, Gratzel M (1991) Nature 353:373
2. Huang SY, Kavan L, Gratzel M, Exnar I (1995) J Electrochem Soc 142:142
3. Wang Z, Hu X (1999) Thin Solid Films 352:62
4. Deb SK (1973) Philos Mag 27:801
5. Granqvist CG (1995) Handbook of inorganic electrochromic materials. Elsevier, Amsterdam
6. Weinberger R, Garber RB (1995) Appl Phys Lett 66:2409
7. Manno D, Micocci G, Rella R, Serra A, Taurino A, Tepore A (1997) J Appl Phys 82:54
8. Granqvist CG (1991) Appl Phys 52:83
9. Ohtsuka T, Masuda M, Sato N (1987) J Electrochem Soc 134:2406
10. Dinh NN, Oanh NTT, Long PD, Bernard MC, Goff AH-L (2003) Thin Solid Films 423:70
11. Lu W, Feng L, Cao G, Jiao Z (2004) J Mater Sci 39:3523
12. Hoffmann S, Waser R (1999) J European Ceram Soc 19:1339
13. Kao MC, Chen HZ, Wang CM, Chen YC, Lee MS (2004) Appl Phys A 79:103
14. Hsieh PT, Chen YC, Wang CM, Tsai YZ, Hu CC (2006) Appl Phys A 84:345
15. Chao HE, Yun YU, Xingfang HU, Larbot A (2003) J Eur Ceram Soc 23:1457
16. Sen S, Mahanty S, Roy S, Heintz O, Bourgeois S, Chaumont D (2005) Thin Solid Films 474:245
17. Natarajan C, Nogami G (1996) J Electrochem Soc 143:1549
18. Tu YL, Milne SJ (1995) J Mater Sci 30:2507
19. Ozer N (1992) Thin Solid Films 214:17
20. Wang CM, Lin SY (2006) J Solid State Electrochem 10:255
21. He JL, Chiu MC (2000) Surf Coat Tech 127:43
22. Hutchins MG, Kamel NA, Abdel-Hady K (1998) Vacuum 51:433
23. Anwar M, Hogarth CA (1988) Phys Stat Sol 109:469
24. Gorenstein A, Scarminio J, Lourenco A (1996) Solid State Ion 86–88:977
25. Rougier A, Portemer F, Quede A, Marssi ME (1999) Appl Surf Sci 153:1
26. Papaefthimiou S, Leftheriotis G, Yianoulis P (2000) Electrochem Acta 46:2145
27. Wang Z, Hu X (2001) Electrochim Acta 46:1951
28. Wang CM, Lin SY, Chen YC (2007) J Phys Chem Solids (in press)